

# Enhancing SMM properties in a family of [Mn<sub>6</sub>] clusters†

Constantinos J. Milios,<sup>a</sup> Ross Inglis,<sup>a</sup> Rashmi Bagai,<sup>b</sup> Wolfgang Wernsdorfer,<sup>c</sup> Anna Collins,<sup>a</sup> Stephen Moggach,<sup>a</sup> Simon Parsons,<sup>a</sup> Spyros P. Perlepes,<sup>d</sup> George Christou<sup>b</sup> and Euan K. Brechin<sup>\*a</sup>

Received (in Cambridge, UK) 5th April 2007, Accepted 17th May 2007

First published as an Advance Article on the web 25th June 2007

DOI: 10.1039/b705170k

The complex [Mn<sub>6</sub>O<sub>2</sub>(Et-sao)<sub>6</sub>(O<sub>2</sub>C<sub>11</sub>H<sub>15</sub>)<sub>2</sub>(EtOH)<sub>6</sub>] has  $U_{\text{eff}} = 80$  K.

For some time, we have been attempting to make polymetallic clusters of transition metal ions with the purpose of synthesizing single-molecule magnets (SMMs).<sup>1</sup> Our approach, like many others,<sup>2</sup> was to employ flexible organic bridging ligands in self-assembly processes and was particularly focused on using manganese. One such project involved the coordination chemistry of salicylaldoxime (saoH<sub>2</sub>).<sup>3</sup> In all of the Mn clusters we isolated and analysed we noticed that, without exception, the exchange between the metal centres was very weak and typically only a few wavenumbers (<1–2 cm<sup>-1</sup>) in magnitude. This is exemplified by the hexametallc SMM [Mn<sub>6</sub>O<sub>2</sub>(sao)<sub>6</sub>(O<sub>2</sub>CH<sub>2</sub>(EtOH)<sub>4</sub>].<sup>4</sup> Normally this would be considered a disadvantage since it inevitably leads to a ground state that is not well isolated from its excited states. However, it also means that the switching from an antiferromagnetic exchange interaction to a ferromagnetic exchange interaction becomes easier to achieve—especially since only minor structural modifications can lead to major changes in  $|J|$ .<sup>5</sup> One possible way of achieving such a switch is to structurally distort the molecule in question, either *via* ‘external’ means, (*i.e.* the application of pressure<sup>6</sup>), or ‘internally’ *via* deliberate chemical modification of the magnetic core. We speculated<sup>7</sup> that the latter strategy would bear fruit in the case of the [Mn<sub>6</sub>O<sub>2</sub>(sao)<sub>6</sub>(O<sub>2</sub>CR)<sub>2</sub>(EtOH)<sub>4</sub>] family ( $S = 4$ )<sup>8</sup> if the Mn–O–N–Mn torsion angles of the bridging salicylaldoximate ligands could be sufficiently ‘twisted’. We achieved this by derivatising the oximate carbon atom with ‘bulky’ Me (Me–saoH<sub>2</sub>), Et (Et–saoH<sub>2</sub>) and Ph (Ph–saoH<sub>2</sub>) groups and re-making the analogous, but more sterically ‘hindered’ hexametallc clusters. For example, the complex [Mn<sub>6</sub>O<sub>2</sub>(Et–sao)<sub>6</sub>(O<sub>2</sub>CPh)<sub>2</sub>(EtOH)<sub>4</sub>(H<sub>2</sub>O)<sub>2</sub>] (**1**) has an  $S = 12$  ground state,<sup>7a</sup> while complex [Mn<sub>6</sub>O<sub>2</sub>(Et–sao)<sub>6</sub>(O<sub>2</sub>CPh(Me)<sub>2</sub>)<sub>2</sub>(EtOH)<sub>6</sub>] (also with an  $S = 12$  ground state)<sup>7b</sup>—has a record value of the effective barrier to magnetization reversal ( $U_{\text{eff}}$ ) of 86.4 K. Here we demonstrate the general applicability of this approach to the [Mn<sub>6</sub>O<sub>2</sub>(R–sao)<sub>6</sub>(O<sub>2</sub>CR)<sub>2</sub>L<sub>6</sub>] class of SMMs by reporting new members of this family which show either similar, or larger, effective energy barriers than the

[Mn<sub>12</sub>O<sub>12</sub>(O<sub>2</sub>CCH<sub>2</sub>Br)<sub>16</sub>(H<sub>2</sub>O)<sub>4</sub>] (Mn<sub>12</sub>–BrAc)<sup>9</sup> member of the prototype [Mn<sub>12</sub>] family. We also speculate that the antiferromagnetic (AF) to ferromagnetic (F) transition in the exchange occurs at a Mn–N–O–Mn torsion angle of ~31°, and that the bigger this angle the more positive (F) the exchange becomes.

The complexes [Mn<sub>6</sub>O<sub>2</sub>(Et–sao)<sub>6</sub>(O<sub>2</sub>CPhMe)<sub>2</sub>(EtOH)<sub>4</sub>(H<sub>2</sub>O)<sub>2</sub>] (**2**) and [Mn<sub>6</sub>O<sub>2</sub>(Et–sao)<sub>6</sub>(O<sub>2</sub>C<sub>11</sub>H<sub>15</sub>)<sub>2</sub>(EtOH)<sub>6</sub>] (**3**), (where HO<sub>2</sub>CPhMe = 4-methyl-benzoic acid; HO<sub>2</sub>C<sub>11</sub>H<sub>15</sub> = adamantane carboxylic acid) can be made in excellent yields from the simple combination of Mn(ClO<sub>4</sub>)<sub>2</sub>·4H<sub>2</sub>O, the corresponding derivatized oxime, Et<sub>4</sub>NOH (or CH<sub>3</sub>ONa) and the appropriate HO<sub>2</sub>CR in EtOH. The three complexes (**1**–**3**) are isostructural: each (Fig. 1 shows complex **3**) consists of two off-set [Mn<sub>3</sub>O]<sup>7+</sup> triangles linked together *via* two oximate oxygen atoms from two η<sup>1</sup>:η<sup>2</sup>:η<sup>1</sup>:μ<sub>3</sub> Et–sao<sup>2-</sup> ligands and two phenolate oxygen atoms derived from two η<sup>2</sup>:η<sup>1</sup>:η<sup>1</sup>:μ<sub>3</sub> Et–sao<sup>2-</sup> ligands. The remaining two oximate(–2) ligands each bridges one edge of a [Mn<sub>3</sub>O]<sup>7+</sup> triangle in an η<sup>1</sup>:η<sup>1</sup>:η<sup>1</sup>:μ fashion thus forming a [Mn<sub>6</sub>O<sub>2</sub>(μ<sub>3</sub>-O)<sub>2</sub>(μ<sub>3</sub>-ONR)<sub>2</sub>(μ-ONR)<sub>4</sub>(μ-OR')<sub>2</sub>]<sup>6+</sup> core. The remaining coordination sites on the Mn ions are filled by terminally coordinated carboxylates and alcohols (or a combination of alcohol/H<sub>2</sub>O). Each 6-coordinate Mn ion is in distorted octahedral geometry with the Jahn–Teller axes all approximately perpendicular to the [Mn<sub>3</sub>] planes. There is only one major intramolecular structural difference between all three complexes (**1**–**3**)—the degree of twisting in the Mn–N–O–Mn linkage along each edge of the Mn<sub>3</sub> triangles. These torsion angles are summarized in Table 1 and Fig. 1, and range from a minimum value of 30.4° to 47.2°. **1**–**3** all crystallize in the triclinic space group  $P\bar{1}$  as **1**·2EtOH, **2**·2EtOH, and **3**. In each case the molecules have only one orientation in the crystal, with neighbouring molecules stacked directly upon each other in a head-to-tail fashion. For **1** and **2** the solvate molecules sit between

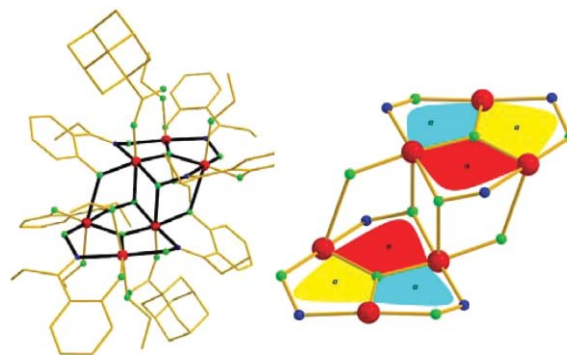


**Fig. 1** Molecular structure of **3** and the [Mn<sub>6</sub>O<sub>2</sub>(NOR)<sub>6</sub>(OR')<sub>2</sub>]<sup>6+</sup> core common to **1**–**3** highlighting the Mn–N–O–N torsion angles ( $\alpha$ ). Atom colour code: Mn = red, O = green, N = blue, C = yellow.

<sup>a</sup>School of Chemistry, The University of Edinburgh, West Mains Road, Edinburgh, EH9 3JJ, UK. E-mail: ebrechin@staffmail.ed.ac.uk; Tel: 0131-650-7545

<sup>b</sup>Chemistry Department, University of Florida, Gainesville, Florida, 32611-7200, USA

<sup>c</sup>Laboratoire Louis Néel-CNRS, 38042 Grenoble, Cedex 9, France

<sup>d</sup>Department of Chemistry, University of Patras, 26504, Patras, Greece

† Electronic supplementary information (ESI) available: Exchange interaction schemes for complexes **1**–**3** and susceptibility measurements for **3**. See DOI: 10.1039/b705170k

**Table 1** Structural and magnetic parameters for complexes 1–3

	Crystal system	Torsion angles $\alpha/^\circ$	$J/\text{cm}^{-1}$	$S$	$g$	$D/\text{cm}^{-1}$	$\tau_0/\text{s}$	$U_{\text{eff}}/\text{K}$
(1)	Triclinic	31.3, 38.2, 39.9	+0.93	12	1.99	-0.43	$8.0 \times 10^{-10}$	53.1
(2)	Triclinic	30.4, 38.2, 47.2	+1.85/-0.70	12	2.00	-0.34	$7.5 \times 10^{-10}$	69.9
(3)	Triclinic	34.0, 36.7, 42.6	+1.60	12	1.99	-0.43	$2.5 \times 10^{-10}$	79.9

head and tail with each  $[\text{Mn}_6]$  complex forming a total of four intermolecular H-bonds to these molecules propagated through the terminal O-atom of the  $\eta^1:\eta^1:\eta^1:\mu$  oximate ligand, essentially creating one dimensional 'zig-zag' chains of  $[\text{Mn}_6]$  clusters. For **3**, in which there are no solvate molecules in the lattice, the only H-bonds are of the intramolecular variety, between terminally bound alcohol/water molecules and the unbound arm of the carboxylate.

Dc and ac susceptibility measurements for all three complexes provide very similar data, best-fit parameters of which are summarized in Table 1. Fig. 2 shows the  $\chi_M T$  vs  $T$  data for all three complexes, with the inset showing representative magnetization data, obtained for complex **3**. Dc susceptibility measurements in a 0.1 T applied field show a continuous rise from a room temperature value of  $\sim 20 \text{ cm}^3 \text{ K mol}^{-1}$  at 300 K to a maximum of approximately  $70 \text{ cm}^3 \text{ K mol}^{-1}$  at 5 K for **1** and **3**, and  $60 \text{ cm}^3 \text{ K mol}^{-1}$  for **2**. For **1** and **3** the data can be satisfactorily simulated using a simple  $1J$ -model (Figure SI1, Table 1) employing the Hamiltonian  $\hat{H} = -2J (\hat{S}_1 \cdot \hat{S}_2 + \hat{S}_2 \cdot \hat{S}_3 + \hat{S}_1 \cdot \hat{S}_3 + \hat{S}_1' \cdot \hat{S}_2' + \hat{S}_2' \cdot \hat{S}_3' + \hat{S}_1' \cdot \hat{S}_3' + \hat{S}_3 \cdot \hat{S}_1' + \hat{S}_1 \cdot \hat{S}_3')$  to reveal the presence of weak ferromagnetic exchange between the metal centers, and  $S = 11$  excited states lying  $\sim 5 \text{ cm}^{-1}$  above the  $S = 12$  ground states, in both cases. Using the same model, the data for **2** can be simulated—but only rather poorly, and can be improved greatly by introducing the  $2J$ -model shown in Figure SI2 and assuming that the interaction between Mn1 and Mn3 (and symmetry equivalents) mediated by an Mn–N–O–Mn torsion angle of  $30.4^\circ$  is antiferromagnetic. This leads to an  $S = 12$  ground state with the  $S = 11$  first excited state only  $1.4 \text{ cm}^{-1}$  higher in energy (Table 1). In theory all three complexes could be simulated with a 2 or 3 $J$  model, but for **1** and **3** this does nothing to enhance the simulation. From the susceptibility data it appears that the more positive

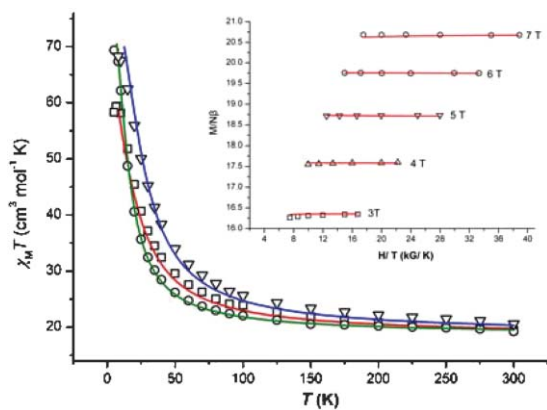


**Fig. 2** Plot of  $\chi_M T$  versus  $T$  for 1–3, the solid lines represent simulations of the data for **1** (green), **2** (red) and **3** (blue); inset: plot of reduced magnetization ( $M/N\beta$ ) versus  $H/T$  for **3**. The solid lines represent a fit of the data.

$J$ -values equate to the largest Mn–N–O–Mn torsion angles (Table 1).

Variable temperature, variable field dc magnetization data were collected in the ranges 1.8–6 K and 0.5–7 T. In each case we fitted the data using a matrix-diagonalization method to a model that assumes only the ground-state is populated, includes axial zero-field splitting ( $D\hat{S}_z^2$ ), and carries out a full powder average (the corresponding Hamiltonian is given by  $\hat{H} = D\hat{S}_z^2 + g\mu_B\mu_0\hat{S}\cdot H$  where  $D$  is the axial anisotropy,  $\mu_B$  is the Bohr magneton,  $\mu_0$  is the vacuum permeability,  $\hat{S}_z$  is the easy-axis spin operator, and  $H$  is the applied field). The fits reveal (Table 1) each cluster to have an  $S = 12$  ground state with axial zfs parameters in the range  $0.34 \leq |D| \leq 0.43 \text{ cm}^{-1}$ . Ac susceptibility measurements were performed on all complexes in the temperature range 1.8–15 K in zero applied dc field and a 3.5 G ac field oscillating at 5–1500 Hz. For each complex the in-phase ( $\chi_M'$ , plotted as  $\chi_M' T$  vs  $T$  for **3** in Fig. SI3) signal displays a plateau at a value of approximately  $75 \text{ cm}^3 \text{ K mol}^{-1}$  at temperatures above  $\sim 8$  K. This value is consistent with an  $S = 12$  ground state ( $78 \text{ cm}^3 \text{ K mol}^{-1}$ ). The signals display a frequency-dependent decrease below  $\sim 8$  K with a concomitant increase in the out-of-phase ( $\chi_M''$ ) signal (Fig. 3). At a frequency of 1500 Hz the  $\chi_M''$  peak maximum for complex **3**

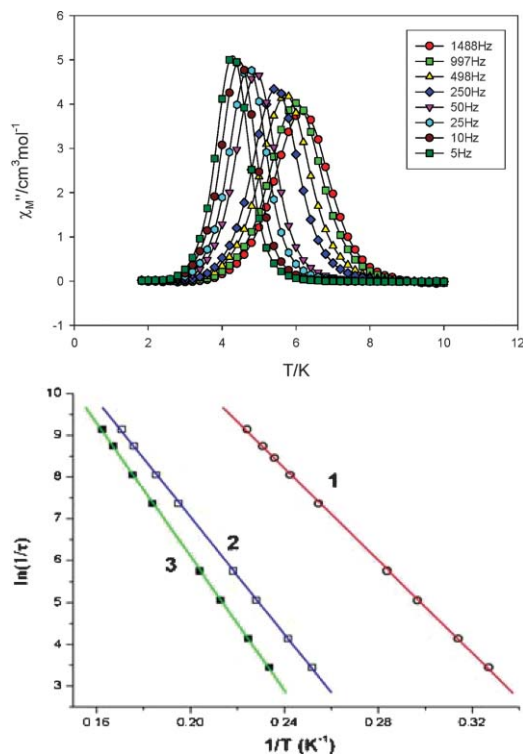


**Fig. 3** Out-of-phase ( $\chi_M''$ ) ac susceptibility measurements for **3** at the indicated temperatures and frequencies (top); Arrhenius plot using the ac data for complexes 1–3. The solid lines are a fit of the data—see text and Table 1 for details (bottom).

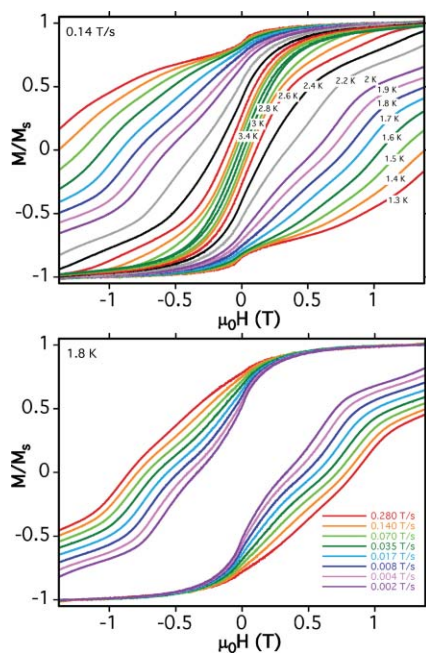


**Fig. 4** Magnetization versus field hysteresis loops for a single crystal of **2** at the indicated temperatures and field sweep rates (bottom).  $M$  is normalised to its saturation value.

occurs at approximately 6 K. The resulting Arrhenius plots using the ac data are shown in Fig. 3. In order to more accurately determine the energy barriers for magnetization reversal, the ac  $\chi_M''$  data for each complex were used in combination with single crystal dc decay measurements performed on single crystals using a micro-SQUID apparatus.<sup>10</sup> The combined data were then used to construct Arrhenius plots, with fits of the thermally activated regions affording the  $\tau_0$  and  $U_{\text{eff}}$  values shown in Table 1. Hysteresis loops were observed for single crystals of **1–3** whose coercivity was strongly temperature and sweep-rate dependent. Loops for complex **2** are given in Fig. 4, and display hysteresis up to approximately 3.5 K at a 0.14 mT s<sup>-1</sup> sweep rate. Each of the loops exhibit well defined steps due to the rapid relaxation of the magnetization at a given magnetic field. However in each case the loops are rather complicated: step positions arising from the ground state transitions are difficult to assign, and it is clear that many additional features are present. These additional steps probably originate from resonant tunneling between  $M_S$ -levels of the ground state, which are shifted to other fields due to fourth order anisotropy terms,<sup>11</sup> or from tunneling between levels of the ground state and low lying excited spin states.

This is perhaps not surprising given that in each case the susceptibility studies suggested the presence of low lying excited states in close proximity to the ground state, presumably as a consequence of the weak exchange between the metal centers. The result is therefore the unavoidable population of excited states even at very low temperatures. The presence of intermolecular interactions (H-bonded solvate molecules) in the crystal and the low molecular and crystallographic symmetry will also affect the loops but their relative significance to the tunneling is difficult to quantify. For  $\text{Mn}_{12}\text{-OAc}$  the role of the solvent has been shown to be of crucial importance,<sup>12</sup> but whether this is also the case here is unclear and will require the synthesis and analysis of analogous

compounds. In conclusion, we have demonstrated the general applicability of ‘targeted structural distortion’ as a method for obtaining high spin molecules with enhanced SMM properties. In this case the replacement of  $\text{PhCO}_2^-$  by the bulkier  $\text{MePhCO}_2^-$  and  $\text{C}_{10}\text{H}_{15}\text{CO}_2^-$  ligands has provided two SMMs with large anisotropy barriers. In order to obtain insight into structure-property relationships it is always necessary to obtain a large body of experimental evidence. In our case initial studies on the first few members of the  $\text{Mn}_6$  family suggest a correlation between Mn–O–N–Mn torsion angles,  $J$ -values and  $U_{\text{eff}}$ . That is, the bigger the torsion angle, the larger (more positive) the exchange, and the larger the  $U_{\text{eff}}$ . Synthetic efforts to obtain yet more members of this family of SMMs in order to establish a magneto-structural correlation are underway.‡

## Notes and references

‡ Anal. calcd (found) for dried **2** solvent free: C 51.16 (51.08), H 5.28 (5.19), N 4.59 (4.66). **3**: Anal. calcd (found) for **3**: C 53.50 (50.56), H 6.12 (6.08), N 4.25 (4.20). Crystal data for **2**:  $\text{C}_{82}\text{H}_{108}\text{Mn}_6\text{N}_6\text{O}_{26}$ ,  $M = 1923.95 \text{ g mol}^{-1}$ ,  $T = 150 \text{ K}$ , triclinic  $P\bar{1}$ ,  $a = 12.6159(3) \text{ \AA}$ ,  $b = 13.0159(2) \text{ \AA}$ ,  $c = 14.5850(3) \text{ \AA}$ ,  $\alpha = 105.6790(10)^\circ$ ,  $\beta = 92.6250(10)^\circ$ ,  $\gamma = 105.1690(10)^\circ$ ,  $V = 2207.95(8) \text{ \AA}^3$ ,  $d_{\text{calcd}} = 1.446 \text{ g cm}^{-3}$ , independent reflections 10575 [ $R(\text{int}) = 0.035$ ], parameters 541, final  $R1 = 0.0366$  for 7652 reflections with  $F > 4\sigma(F)$ . Crystal data for **3**:  $\text{C}_{88}\text{H}_{120}\text{Mn}_6\text{N}_6\text{O}_{24}$ ,  $M = 1974.46 \text{ g mol}^{-1}$ ,  $T = 150 \text{ K}$ , triclinic  $P\bar{1}$ ,  $a = 12.7121(4) \text{ \AA}$ ,  $b = 13.1980(4) \text{ \AA}$ ,  $c = 15.2785(5) \text{ \AA}$ ,  $\alpha = 75.593(2)^\circ$ ,  $\beta = 78.672(2)^\circ$ ,  $\gamma = 68.389(2)^\circ$ ,  $V = 2292.53(13) \text{ \AA}^3$ ,  $d_{\text{calcd}} = 1.418 \text{ g cm}^{-3}$ , independent reflections 12813 [ $R(\text{int}) = 0.040$ ], parameters 597, final  $R1 = 0.0428$  for 8631 reflections with  $F > 4\sigma(F)$ . CCDC 636071–636072. For crystallographic data in CIF or other electronic format see DOI: 10.1039/b705170k

- (a) E. K. Brechin, *Chem. Commun.*, 2005, 2141; (b) G. Christou, *Polyhedron*, 2005, **24**, 2065; (c) G. Christou, D. Gatteschi, D. N. Hendrickson and R. Sessoli, *MRS Bull.*, 2000, **25**, 66; (d) D. Gatteschi and R. Sessoli, *Angew. Chem., Int. Ed.*, 2003, **42**, 268; (e) R. Bircher, G. Chaboussant, C. Dobe, H. U. Güdel, S. T. Ochsenbein, A. Sieber and O. Waldmann, *Adv. Funct. Mater.*, 2006, **16**, 209.
- G. Aromí and E. K. Brechin, *Struct. Bonding*, 2006, **122**, 1 and references therein.
- (a) C. J. Milios, PhD Thesis, University of Patras, Greece, 2004; (b) T. C. Stamatas, D. Foguet-Albiol, C. C. Stoumpos, C. P. Raptopoulou, A. Terzis, W. Wernsdorfer, S. P. Perlepes and G. Christou, *J. Am. Chem. Soc.*, 2005, **127**, 15380.
- C. J. Milios, A. Vinslava, A. Whittaker, S. Parsons, W. Wernsdorfer, G. Christou, S. P. Perlepes and E. K. Brechin, *Inorg. Chem.*, 2006, **45**, 5272.
- O. Kahn, *Molecular Magnetism*, Wiley-VCH, 1993.
- A. Sieber, R. Bircher, O. Waldmann, G. Carver, G. Chaboussant, H. Mutka and H. U. Güdel, *Angew. Chem., Int. Ed.*, 2005, **44**, 4239 and references therein.
- (a) C. J. Milios, A. Vinslava, P. Wood, S. Parsons, W. Wernsdorfer, G. Christou, S. P. Perlepes and E. K. Brechin, *J. Am. Chem. Soc.*, 2007, **129**, 8; (b) C. J. Milios, A. Vinslava, W. Wernsdorfer, S. Moggach, S. Parsons, S. P. Perlepes, G. Christou and E. K. Brechin, *J. Am. Chem. Soc.*, 2007, **129**, 2754.
- C. J. Milios, C. P. Raptopoulou, A. Terzis, F. Lloret, R. Vicente, S. P. Perlepes and A. Escuer, *Angew. Chem., Int. Ed.*, 2004, **43**, 210.
- N. E. Chakov, S.-C. Lee, A. G. Harter, P. L. Kuhns, A. P. Reyes, S. O. Hill, N. S. Dalal, W. Wernsdorfer, K. A. Abboud and G. Christou, *J. Am. Chem. Soc.*, 2006, **128**, 6975.
- W. Wernsdorfer, *Adv. Chem. Phys.*, 2001, **118**, 99.
- W. Wernsdorfer, M. Murugesu and G. Christou, *Phys. Rev. Lett.*, 2006, **96**, 057208.
- (a) A. Cornia, R. Sessoli, L. Sorace, D. Gatteschi, A. L. Barra and C. Daugebonne, *Phys. Rev. Lett.*, 2002, **89**, 257201; (b) S. Takahashi, R. S. Edwards, J. M. North, S. Hill and N. S. Dalal, *Phys. Rev. B*, 2004, **70**, 094429.